

NUCLEAR DATA AND MEASUREMENTS SERIES

ANL/NDM-9

**Method of Neutron Activation Cross Section Measurement
for $E_n = 5.5-10$ MeV using the $D(d,n)^3\text{He}$ Reaction as a Neutron Source**

by

D.L. Smith and J.W. Meadows

August 1974

**ARGONNE NATIONAL LABORATORY,
ARGONNE, ILLINOIS 60439, U.S.A.**

NUCLEAR DATA AND MEASUREMENTS SERIES

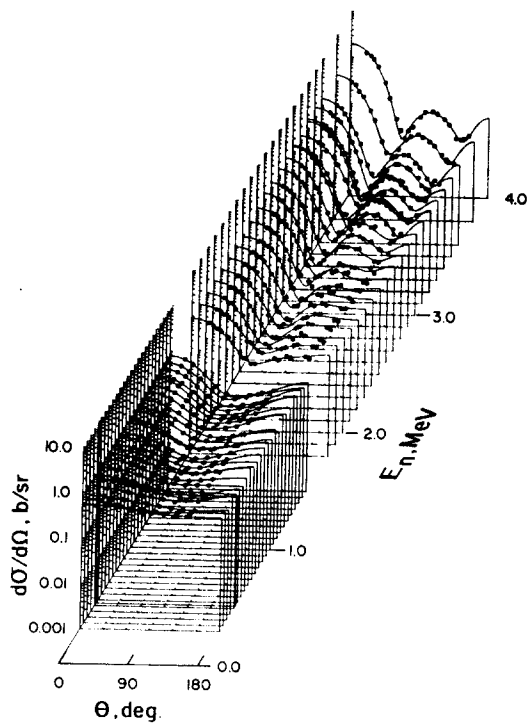
ANL/NDM - 9

METHOD OF NEUTRON ACTIVATION CROSS SECTION
MEASUREMENT FOR $E_n = 5.5-10$ MeV USING
THE $D(d,n)He-3$ REACTION AS A NEUTRON SOURCE

by

D. L. Smith and J. W. Meadows

August 1974



U of C - AUA - USAEC

ARGONNE NATIONAL LABORATORY,
ARGONNE, ILLINOIS 60439, U.S.A.

The facilities of Argonne National Laboratory are owned by the United States Government. Under the terms of a contract (W-31-109-Eng-38) between the U. S. Atomic Energy Commission, Argonne Universities Association and The University of Chicago, the University employs the staff and operates the Laboratory in accordance with policies and programs formulated, approved and reviewed by the Association.

MEMBERS OF ARGONNE UNIVERSITIES ASSOCIATION

The University of Arizona
Carnegie-Mellon University
Case Western Reserve University
The University of Chicago
University of Cincinnati
Illinois Institute of Technology
University of Illinois
Indiana University
Iowa State University
The University of Iowa

Kansas State University
The University of Kansas
Loyola University
Marquette University
Michigan State University
The University of Michigan
University of Minnesota
University of Missouri
Northwestern University
University of Notre Dame

The Ohio State University
Ohio University
The Pennsylvania State University
Purdue University
Saint Louis University
Southern Illinois University
The University of Texas at Austin
Washington University
Wayne State University
The University of Wisconsin

NOTICE

This report was prepared as an account of work sponsored by the United States Government. Neither the United States nor the United States Atomic Energy Commission, nor any of their employees, nor any of their contractors, subcontractors, or their employees, makes any warranty, express or implied, or assumes any legal liability or responsibility for the accuracy, completeness or usefulness of any information, apparatus, product or process disclosed, or represents that its use would not infringe privately-owned rights.

ANL/NDM - 9

METHOD OF NEUTRON ACTIVATION CROSS SECTION
MEASUREMENT FOR $E_n = 5.5-10$ MeV USING
THE $D(d,n)He-3$ REACTION AS A NEUTRON SOURCE

by

D. L. Smith and J. W. Meadows

August 1974

Applied Physics Division
Argonne National Laboratory
9700 South Cass Avenue
Argonne, Illinois 60439
U.S.A.

NUCLEAR DATA AND MEASUREMENTS SERIES

The Nuclear Data and Measurements Series presents results of studies in the field of microscopic nuclear data. The primary objective is the dissemination of information in the comprehensive form required for nuclear technology applications. This Series is devoted to: a) Measured microscopic nuclear parameters, b) Experimental techniques and facilities employed in data measurements, c) The analysis, correlation and interpretation of nuclear data, and d) The evaluation of nuclear data. Contributions to this Series are reviewed to assure a high technical excellence and, unless otherwise stated, the contents can be formally referenced. This Series does not supplant formal journal publication but it does provide the more extensive information required for technological applications (e.g. tabulated numerical data) in a timely manner.

TABLE OF CONTENTS

	<u>Page</u>
ABSTRACT.	3
I. INTRODUCTION	4
II. EXPERIMENTAL PROCEDURES.	5
A. Apparatus	5
B. Neutron Irradiations.	7
III. ACTIVATION DATA PROCESSING	8
A. General	8
B. Neutron Source Representation	8
C. Computation of Reaction Cross Sections.	11
D. Neutron Scattering from the Target.	16
IV. SOME NUMERICAL RESULTS	16
V. CONCLUSIONS.	17

METHOD OF NEUTRON ACTIVATION CROSS SECTION MEASUREMENT
FOR $E_n = 5.5 - 10$ MeV USING THE $D(d,n)He-3$
REACTION AS A NEUTRON SOURCE

by

D. L. Smith and J. W. Meadows

ABSTRACT

Neutron cross section measurements for $E_n = 5.5 - 10$ MeV can be effectively performed using the $D(d,n)He-3$ reaction as a source of predominantly monoenergetic neutrons. Relatively intense neutron production has been achieved using deuteron beams from the Argonne National Laboratory Fast Neutron Generator (FNG) in conjunction with a deuterium gas cell target. The objective of this report is to describe the experimental and data analysis procedures which are employed in a program of neutron activation cross section measurements in this energy region.

I. INTRODUCTION

Nuclear reactions of the type (n,γ) , $(n;n'\gamma)$, (n,p) , $(n;p,n)$, (n,d) , (n,α) , $(n;\alpha,n)$ and $(n,2n)$ produced by fast neutrons influence the neutronics of fission reactors and proposed fusion systems and are instrumental in generation of heat and radiation damage in the structural materials. Several reactions in this category are commonly used as standards in neutron dosimetry. The cross sections of many of these reactions in important structural materials are not adequately known for applications [1]. The byproducts from a number of reactions are radioactive and cross sections can be derived from measurements of the activities. A program of these measurements is being conducted at the Argonne Fast Neutron Generator (FNG) facility.

The experimental and data analysis procedures for measurements made with $E_n < 6$ MeV using the ${}^7\text{Li}(p,n){}^7\text{Be}$ reaction as a neutron source are described in considerable detail in a recent report [2]. Limitations in available beam energy and complexity of the neutron spectrum from a lithium target for $E_p \gtrsim 7.5$ MeV prevent use of this reaction for measurements with $E_n > 6$ MeV.

Measurements in the region $E_n = 5.5 - 10$ MeV can be performed using the $\text{D}(d,n)\text{He-3}$ reaction as a neutron source. This reaction is exoergic ($Q = + 3.269$ MeV) and yields a single neutron-energy group. For $E_d > 4.45$ MeV additional neutrons are produced via the $\text{D}(d;n,p)\text{D}$ reaction ($Q = - 2.225$ MeV). Neutrons from the latter reaction are not monoenergetic and their presence complicates the data analysis process.

The $\text{D}(d,n)\text{He-3}$ neutron source reaction has been reviewed and evaluated by Liskien and Paulsen [3] and results from their paper are utilized in the present work. Unfortunately, very little data is available on the neutron spectrum

associated with $D(d;n,p)D$ reaction. It was apparent at the outset that the presence of these breakup neutrons could have a significant effect on the measurement of neutron activation cross sections for $E_n = 8.5 - 10$ MeV. Therefore, we made time-of-flight measurements of the neutron yield from the $D(d;n,p)D$ reaction relative to the neutron group from the $D(d,n)He-3$ reaction at zero degrees for $E_d = 5.278, 5.937, 6.302, 6.709$ and 7.219 MeV. We also measured the angular distribution functions for $\theta < 30^\circ$ at $E_d = 6.709$ and 7.219 MeV. These data were used to correct the activation cross sections for $D(d;n,p)D$ neutrons.

In many respects, the experimental and data analysis procedures are independent of the neutron source reaction employed. Sample materials are irradiated along with a fission chamber monitor which measures the integrated neutron dose. The sample activity is measured utilizing a calibrated detector. The reader is referred to Ref. 2 for descriptions of half life corrections, detector calibrations, neutron multiple scattering and other details which are not strongly dependent on the neutron source.

The present report is limited to discussion of those experimental and data analysis procedures which are unique to the use of the $D(d,n)He-3$ reaction in the neutron activation measurements program.

II. EXPERIMENTAL PROCEDURES

A. Apparatus

We use a gas target assembly for our measurements rather than the alternative deuterated metal targets. Although deuterated metal targets are stable, easy to use and provide a point neutron source the neutron yield per MeV energy loss of the deuterons is smaller because much of the energy is dissipated by ionizing the metal atoms. Gas cells provide much

better energy definition for the same neutron yield but the source is a line rather than a spot and the target is troublesome to use because the entrance window is easily punctured causing loss of deuterium gas and flight tube vacuum. Background neutrons produced via (d,n) reactions in the structure of both targets and particularly in the carbon deposits that form with use were the decisive factor in the choice of targets. This background can be readily measured for a gas target by evacuating the cell. This is not possible with a deuterated metal target.

Fig. 1 is a schematic diagram of the gas target assembly and fission chamber employed for sample irradiations. The operation of the fission chamber is described in Ref. 2. Measurements for $E_n = 5.5 - 10$ MeV are made using a uranium deposit enriched in U-238 so that the neutron monitor will be less sensitive to low-energy neutrons ($E_n \lesssim 1$ MeV). The incident deuteron beam passes through a thin nickel foil (~ 2 milligrams/cm² thick) into the gas cell which is ~ 2 cm long and contains deuterium gas at ~ 2 atmospheres pressure (~ 28 p.s.i. absolute). The nickel foil is backed by a grid which aids in its support and cooling. A vacuum seal is achieved by epoxying the edge of the foil to a water-cooled flange. Portions of the gas target assembly which are exposed to the deuteron beam (except for the nickel foils) are gold plated to minimize neutron background from (d,n) reactions in Fe, Cu, Zn and other relatively low-Z constituents of the cell.

A deuterium gas handling system (not shown in Fig. 1) is used to evacuate the gas cell and fill it with deuterium to the desired pressure. The cell pressure can be monitored during exposures to detect slow leaks or sudden puncture of the foil by the deuteron beam. The nickel foils do not tolerate a well-focused beam from the FNG facility at normal operating beam current levels. Consequently, the beam is

"diffused" by two crossed 60 Hz magnetic deflectors to a spot $\sim 1 \text{ cm}^2$ on the target grid during exposures.

B. Neutron Irradiations

Neutron irradiations of samples and the monitor are conducted as described in Ref. 2 with the exception of a few procedural differences which will be described in the present report.

Improved gas cell window survival is observed if the nickel foil is "annealed" during each exposure by slowly raising the beam current to its operating level at the start and slowly decreasing it at the end of the exposure. Sudden beam current changes offer a higher risk of window puncture and resultant loss of flight tube vacuum.

In spite of the gold plating on cell components, considerable neutron background is observed from an evacuated cell. We made some time-of-flight measurements of the empty target neutron spectrum which indicate that (d,n) reactions from the nickel foil and from carbon buildup on the vacuum side of the foil and grid are largely responsible for the background.

Background from Ni(d,n) reactions is essentially constant for a specific nickel foil and deuteron beam energy. Thus, background corrections can be experimentally determined by irradiating two samples at each beam energy—one with the gas cell filled with deuterium and one with the cell evacuated. The two exposures are normalized by means of the beam current integrator. Neutron yield from carbon buildup is variable (sensitive to changes in beam optics as well as time). Nevertheless, we have obtained satisfactory results by insuring that the main and background irradiations required for a particular beam energy are made sequentially using the same nickel foil.

Normally, irradiations are made with beam currents of $\sim 10 - 15 \mu\text{A}$ diffused as described above. The fission chamber is placed close to the gas cell ($D \sim 3-5 \text{ cm}$ as shown in Fig. 1) to enhance the neutron dose received by the sample and monitor. Irradiation times vary considerably depending on magnitude of the cross section and half life of the induced activity. Typical values for previous irradiations range from $\sim 5 - 7$ minutes for $\text{Al-27}(n,p)\text{Mg-27}$ activation ($t_{1/2} = 9.5 \text{ min}$) to $\sim 1-2$ hours for $\text{Fe-54}(n,p)\text{Mn-54}$ activation ($t_{1/2} = 312 \text{ days}$).

III. ACTIVATION DATA PROCESSING

A. General

The computations required to convert the raw experimental data to final activation cross sections will be discussed in this section. The concepts are basically the same as described in Ref. 2 and wherever possible, the parameter designations of the present report will be the same as in the earlier report. A reader who wishes to follow the numerical development in detail will find Ref. 2 indispensable because certain figures, tables and formulas appearing in the earlier report are applicable to the present work and will not be repeated here.

B. Neutron Source Representation

We rely on results from the review paper by Liskien and Paulsen [3] for representation of the neutron group from the $\text{D}(d,n)\text{He-3}$ reaction and data from our own work for representation of the additional neutrons from the $\text{D}(d;n,p)\text{D}$ reaction.

Three variables are involved in the description of the neutron current incident upon the sample and monitor: E_d (laboratory energy of the incident deuterons), θ (laboratory emission angle for neutrons relative to the beam axis) and E_n (laboratory energy of the neutrons). For specific E_d

and θ , the $D(d,n)He-3$ reaction yields a discrete neutron group with energy E_{n1} which can be calculated from standard two-body kinematic formulas (e.g. see Eqs. 1-7 of Ref. 4). Neutrons from the $D(d;n,p)D$ reaction have a broader energy spectrum because of the three-body final state. The absolute neutron yield is unimportant since we are analyzing data from relative measurements. On the other hand, the energy spectrum and angular distribution of the emitted neutrons is significant because of geometric considerations and differences in the excitation functions for the monitor and sample reactions.

The $D(d,n)He-3$ neutron current F_1 incident on the sample and monitor can be represented by the formula

$$F_1(E_d, \theta) = C \left. \frac{d\sigma}{d\Omega} \right|_{D(d,n)He-3}(E_d, \theta) \quad (1)$$

where $\left. \frac{d\sigma}{d\Omega} \right|_{D(d,n)He-3}(E_d, \theta) =$ laboratory differential neutron production cross section for the $D(d,n)He-3$ reaction (see Ref. 3)

and C is a normalization constant which can be assumed unity. Liskien and Paulsen [3] represent the center-of-mass differential cross section by the Legendre polynomial expansion

$$\left. \frac{d\sigma}{d\Omega} \right|_{D(d,n)He-3}^{CM}(E_d, \theta_{CM}) = \left. \frac{d\sigma}{d\Omega} \right|_{D(d,n)He-3}^{CM}(E_d, 0^\circ) \sum_{\nu=0}^{\eta} A_\nu(E_d) P_\nu(\cos \theta_{CM}) \quad (2)$$

where $\nu \leq 10$ and the coefficients of the odd-order polynomials are zero. Normalization is such that

$$\sum_{\substack{\nu=0 \\ \text{(even)}}}^{\eta} A_\nu(E_d) = 1 \quad (3)$$

and the zero-degree center-of-mass differential cross section is a multiplicative factor. In the cross section computations we convert from laboratory angle to center-of-mass angle, com-

pute the neutron production cross section via Eq. 2 and convert it to laboratory coordinates to obtain F_1 from Eq. 1. The coordinate transformations are straightforward and unambiguous for an exoergic reaction [5].

The reaction cross section calculations are performed with a digital computer. Several numerical functions are represented by reference tables of discrete values. Linear interpolation or selection of the nearest tabulated values are methods utilized in generating functional values for the calculations. Table I is a set of values for

$$\left. \frac{d\sigma}{d\Omega} \right|_{\text{CM}}^{D(d,n)\text{He-3}} (E_d, 0^\circ)$$

used in the present work. Similarly, values of A_ν appear in Table II.

The neutron spectrum from the $D(d,np)D$ reaction is represented in our work by 16 discrete neutron-energy groups. The neutron yields for each group relative to the $D(d,n)\text{He-3}$ group have been computed for ten laboratory deuteron energies ($E_d = 5.0, 5.278, 5.5, 5.793, 6.0, 6.302, 6.5, 6.709, 7.0$ and 7.219 MeV) and six laboratory angles ($\theta = 2.5, 7.5, 12.5, 17.5, 22.5$ and 27.5 degrees). The $D(d;n,p)D$ neutron yield is negligible for $E_d < 5.0$ MeV. The limit $\theta < 27.5^\circ$ is adequate for our work. For each mean neutron energy, E_{nj} ($j=2, \dots, 17$), there is a neutron energy interval ΔE_{nj} which designates the portion of the continuous spectrum which is lumped into the j th group. Define

$$Y(E_d, \theta, E_n) \equiv \left(\frac{d^2\sigma}{d\Omega dE_n} \right)_{D(d;n,p)D} / \left(\frac{d\sigma}{d\Omega} \right)_{D(d,n)\text{He-3}} \quad (4)$$

in terms of the indicated laboratory differential cross sections. The neutron current for the j th group ($j \geq 2$) is represented by

$$F_j(E_d, \theta) = F_1(E_d, \theta) Y(E_d, \theta, E_{nj}) \Delta E_{nj} \quad (5)$$

with F_1 computed via Eq. 1. Data from our time-of-flight measurements were interpolated to generate values of $Y(E_d, \theta, E_n)$ for the specific E_d and θ listed above. These values appear in Table III.

In Section II.B we mentioned the neutron background from (d,n) reactions on nickel and carbon in the target structure. Since this background is measured and the data is experimentally corrected for it, there is no need to consider it in this section.

C. Computation of Reaction Cross Sections

In order to account for deuteron-beam energy loss in the gas cell as well as geometric effects resulting from the cell length, we divide the cell into N_T layers. If the length of the cell is X_G then each layer has thickness (X_G/N_T) . We define the distance from the front end of the gas cell to the center of the i -th layer as t_{Gi} where

$$t_{Gi} = \frac{X_G}{N_T} (N_T - i + \frac{1}{2}) . \quad (6)$$

Fig. 2 is useful in visualizing the analysis. The deuteron-energy loss in the nickel window and deuterium gas of the cell is a small fraction of the incident deuteron energy for most irradiations. Let

ΔE_{dW} = deuteron-beam energy lost in the nickel window.

ΔE_{dG} = deuteron-beam energy lost in the deuterium gas.

Then the deuteron energy at the i -th target layer is

$$E_{di} = E_{do} - \Delta E_{dW} - \frac{\Delta E_{dG}}{N_T} (i - \frac{1}{2}) \quad (7)$$

when the incident beam energy is E_{do} .

The window energy loss depends on the nickel foil thickness and is given in MeV by the formula

$$\Delta E_{dW} \approx X_W \exp(-0.597 \ln E_{do} - 1.685) \quad (8)$$

where

X_W = Thickness of the nickel window expressed in milligrams/cm².

The energy loss in the gas cell is given in MeV by the formula

$$\Delta E_{dG} \approx X_G (P_G/14.696) \cdot [293.18/(273.18 + T_G)] \cdot \exp[-0.818 \ln (E_{do} - \Delta E_{dW}) - 2.273] \quad (9)$$

where

P_G = deuterium gas pressure in p.s.i. absolute.

T_G = deuterium gas temperature in °C.

We assumed a T_G of 25°C which is probably unrealistic but the results are not too sensitive to this parameter. The ideal gas law was assumed in derivation of Eq. 9.

In order to include neutron attenuation and solid angle effects, the sample is divided into N_S layers of equal thickness. The distance from the i -th target layer to the l -th sample layer is given by the formula

$$d_{Sil} = d + t_{Gi} - X_S \left(1 - \frac{1}{2N_S}\right) + Z_{Sl} \quad (10)$$

where

X_S = sample thickness

d = distance from the gas cell to the fission chamber

$$Z_{Sl} = \frac{X_S}{N_S} (l - 1). \quad (11)$$

The maximum polar angle θ_{Sil}^{\max} for the i -th target layer and l -th sample layer is given by

$$\theta_{Sil}^{\max} = \tan^{-1} (R/d_{Sil}) \quad (12)$$

where

R = radius of the sample and uranium deposit
(≈ 1.27 cm for all measurements).

The maximum polar angle θ_{F1}^{\max} for the i-th target layer and the uranium deposit is given by

$$\theta_{F1}^{\max} = \tan^{-1} [R / (d + t_{G1} + X_B)]. \quad (13)$$

The chamber wall thickness X_B is a negligible factor here.

We divide the angular range $\theta = 0$ to $\theta = \theta_{S1\ell}^{\max}$ into N_D equal polar-angle sectors. The mean angle for the k-th sector is

$$\theta_{S1\ell k} = \frac{\theta_{S1\ell}^{\max}}{N_D} (k - 1/2)^a \quad (14)$$

Similarly for the uranium deposit we obtain

$$\theta_{F1k} = \frac{\theta_{F1}^{\max}}{N_D} (k - 1/2). \quad (15)$$

The activation reaction cross section σ_R can be computed via the formula

$$\sigma_R (E_{nR}) = \frac{(N_A - N_{AB})}{(N_F - N_{FB})} \sigma_{F,235} (E_{nR}) \cdot \left(\sum_{ijk} \mathcal{F}_{ijk} \sum_{ijkl} \mathcal{A}_{ijkl} \right) \quad (16)$$

where

N_A = number of sample atoms activated during the irradiation with a filled gas cell

N_{AB} = number of sample atoms activated during the evacuated cell irradiation.

and similarly N_F and N_{FB} are recorded fissions. $\sigma_{F,235}$ is the U-235 fission cross section. Various corrections for half life, efficiency, branching ratios and coincidence summing are applied where required in obtaining N_A , N_{AB} , N_F and N_{FB} . \mathcal{F}_{ijk} and \mathcal{A}_{ijkl} account for geometric effects, neutron spectrum properties, attenuation, multiple scattering, etc.

The indicated sums are over target layers $1 \leq i \leq N_T$, neutron groups $1 \leq j \leq 17$ (see Section III.B), angles $1 \leq k \leq N_D$ and sample layers $1 \leq \ell \leq N_S$.

a. The factor N_D was inadvertently left out of the denominator of the equivalent Eq. C-4 on Page 39 of Ref. 2.

Although we use a uranium deposit enriched in U-238 for our fission chamber, we choose to express the activation cross section explicitly in terms of the standard U-235 fission cross section in Eq. 16. The fission cross section ratios for U-234, U-236 and U-238 relative to U-235 enter as parameters within the F_{ijk} . These ratios are known with better accuracy than the absolute U-235 fission cross section and the F_{ijk} should not be materially affected by future readjustments of this standard. Therefore, activation cross sections computed by this method can be readily adjusted to reflect future changes in the standard U-235 fission cross section.

The sample correction factors A_{ijkl} can be computed from the formula

$$\begin{aligned}
 A_{ijkl} = & F_{ij}(\theta_{Silk}) \theta_{Sil}^{\max} \sin \theta_{Silk} \exp(-\sum_T Z_{Sl} / \cos \theta_{Silk}) \cdot \\
 & \cdot (n_R / \sum_T X_S) \cdot [\sigma_R^{\text{app}}(E_{nijkl}) / \sigma_R^{\text{app}}(E_{nR})] \cdot \\
 & \cdot [1 - \exp(-\sum_T X_S / \cos \theta_{Silk})] (1 + \alpha_{ij} + \beta_{ij})
 \end{aligned}
 \tag{17}$$

where

n_R = number of appropriate target atoms in the sample

σ_R^{app} = approximate shape of the activation excitation function

\sum_T = macroscopic neutron total cross section for the sample material

α_{ij}, β_{ij} = neutron multiple scattering correction parameters (see Section III.F and Appendices B and C of Ref. 2).

The fission correction factors F_{ijk} can be computed from the formula

$$\begin{aligned}
\mathcal{F}_{ijk} = & F_{ij}(\theta_{Fik})^{\theta_{F1}^{\max}} \tan \theta_{Fik} \cdot \\
& \cdot \exp [-(\sum_{TS} X_S + \sum_{TB} X_B) / \cos \theta_{Fik}] \cdot \\
& \cdot n_U [\sigma_{F,235}(E_{nijk}) / \sigma_{F,235}(E_{nR})] \cdot \\
& \cdot (f_{234} \zeta_{234,235} + f_{235} + f_{236} \zeta_{236,235} + \\
& + f_{238} \zeta_{238,235})(1 + \gamma_{ij} + \rho_{ij}) \quad (18)
\end{aligned}$$

where

n_U = number of uranium atoms in the deposit

f_I = uranium isotope fractions (I=234,235,236,238)

\sum_{TB} = macroscopic neutron total cross section for fission chamber wall.

$\zeta_{I,235}$ = fission cross section ratios for U-234,236,238 relative to U-235.

γ_{ij}, ρ_{ij} = neutron multiple scattering correction parameters (Ref. 2).

The neutron energy E_{nR} selected to correspond to the calculated cross section σ_R is essentially an average energy for the D(d,n)He-3 neutrons incident upon the sample. It is calculated from the formula

$$E_{nR} = \frac{\sum_{ikl} E_{nikl} (A_{ikl} / \Delta E_{nikl})}{\sum_{ikl} (A_{ikl} / \Delta E_{nikl})} \quad (19)$$

where

ΔE_{nikl} = D(d,n)He-3 neutron energy spread for the i th target layer, k th angular interval, and l th sample layer.

The energy resolution assigned to a data point is the total energy spread of D(d,n)He-3 neutrons incident on the

sample. This energy spread arises from target thickness and kinematic effects.

Fission cross sections from Table VII of Ref. 2 are used for the current measurements in the range $E_n = 5.5 - 10$ MeV. These values are from the ENDF/B-III file [6].

D. Neutron Scattering from the Target

Since the gas target assembly is fairly massive it was initially considered a possibility that neutron scattering from the target would noticeably affect the activation cross section measurements. However, it was discovered that the strong forward peaking of the $D(d,n)He-3$ neutrons prevents this from being a serious problem. An estimate of the relative number of scattered and direct neutrons incident upon the sample and monitor was made using a simplified Monte Carlo technique that considers only single scattering. Various neutron cross sections required for the calculations were obtained from the ENDF/B-III file [6]. All inelastic scattering was assumed to be isotropic. The results of a calculation for a typical experimental configuration are given in Table IV. The relative number of scattered neutrons is always $< 2\%$, and since the effects for the sample and monitor tend to cancel, the scattered neutrons are not considered in the cross section data processing.

IV. SOME NUMERICAL RESULTS

Neutron energy resolution for the activation measurements is governed by beam energy losses in the gas target and kinematics of the $D(d,n)He-3$ reaction. Kinematics is the dominant factor. An acceptance angle of 20 degrees produces an energy spread of ~ 0.4 MeV at $E_d = 7$ MeV. Eq. 8 was used to calculate the energy loss ΔE_{dW} for a 2 milligram/cm² nickel window. Eq. 9 was used to calculate the

energy loss ΔE_{dG} for a 2 cm gas cell with a pressure of 2 atmospheres. The results of these calculations appear in Table V. The energy loss in the nickel window exceeds the loss in the gas but not by much.

Background neutrons from (d,n) reactions in the target structure produce a significant fraction of the observed fissions and sample activity as can be seen from the results of typical measurements presented in Table VI. Fortunately, the background is measurable and the corrections can be readily applied to the data. The background is energy dependent so we considered the question of whether the background measured with the cell evacuated is representative of the background produced with deuterium in the cell. The only difference is that the energy of the deuterons incident upon the beam stop is reduced by ~ 0.1 MeV by the presence of the gas. The beam stop is not the primary source of background and even if it were, we can deduce from Table VI that a change of ~ 0.1 MeV in beam energy produces a change of only $\sim 1-2\%$ in the background. Furthermore, the effect upon the cross section is even smaller because of cancellation resulting from similar energy dependence of monitor and sample activation excitation functions.

We rely on knowledge of the neutron spectrum and detailed analysis to correct for the presence of $D(d;n,p)D$ neutrons from the target. The computed cross section is enhanced by the inclusion of $D(d;n,p)D$ neutrons for the representative examples given in Table VII.

V. CONCLUSIONS

We have found that the $D(d,n)He-3$ reaction is a suitable neutron source for activation cross section measurements in the range $E_n = 5.5 - 10$ MeV. In order to obtain acceptable accuracy it is necessary to correct the data for background, geometric effects and neutrons from the $D(d;n,p)D$ reaction.

While the data analysis is tedious, these corrections can be made in a relatively straightforward and reliable manner. There are practical limitations, dictated by yield requirements, to the neutron energy resolution which can be achieved. Most of our measurements have yielded resolutions of $\sim 0.3 - 0.5$ MeV. Fortunately, reaction cross section fluctuations are generally not pronounced for $E_n > 5$ MeV.

References

1. L. Stewart, M. S. Moore and H. T. Motz, "Compilation of Requests for Nuclear Data", Report No. LA-5253-MS (USNDC-6), Los Alamos Scientific Laboratory, Los Alamos, New Mexico 87544 (June 1973).
2. Donald L. Smith and James W. Meadows, "Measurement of $^{58}\text{Ni}(n,p)^{58}\text{Co}$ Reaction Cross Sections for $E_n = 0.44 - 5.87$ MeV Using Activation Methods", Report No. ANL-7989, Argonne National Laboratory, Argonne, Illinois 60439 (August 1973).
3. H. Liskien and A. Paulsen, "Neutron Production Cross Sections and Energies for the Reactions $T(p,n)\text{He-3}$, $D(d,n)\text{He-3}$, and $T(d,n)\text{He-4}$ ", Nuclear Data, Vol. 11, 7 569 (June 1973).
4. A. S. Langsdorf, Jr., J. E. Monahan and W. A. Reardon, "A Tabulation of Neutron Energies from Monoenergetic Protons on Lithium", Report No. ANL-5219, Argonne National Laboratory, Argonne, Illinois 60439 (Jan. 1954).
5. L. I. Schiff, Quantum Mechanics, McGraw-Hill, New York, pp. 96-99 (1955).
6. Evaluated Neutron Data File, ENDF/B-III, National Neutron Cross Section Center, Brookhaven National Laboratory, Upton, New York, USA.

TABLE I

Values of the Center-of-Mass Zero Degree Differential
Neutron Production Cross Section for the D(d,n)He-3 Reaction^a

E_d (MeV)	$\frac{d\sigma}{d\Omega} \Big _{(E_d, 0^\circ)}$ D(d,n)He-3 (barn)	E_d (MeV)	$\frac{d\sigma}{d\Omega} \Big _{(E_d, 0^\circ)}$ D(d,n)He-3 (barn)
0.0	0.0	1.4	0.0227
0.02	0.25×10^{-4}	1.5	0.0234
0.03	0.125×10^{-3}	1.6	0.024
0.04	0.31×10^{-3}	1.7	0.0246
0.05	0.52×10^{-3}	1.8	0.0252
0.06	0.78×10^{-3}	1.9	0.0258
0.07	0.106×10^{-2}	2.0	0.0264
0.08	0.135×10^{-2}	2.1	0.0269
0.09	0.166×10^{-2}	2.2	0.0275
0.1	0.2×10^{-2}	2.3	0.028
0.15	0.333×10^{-2}	2.4	0.0284
0.2	0.46×10^{-2}	2.5	0.0289
0.25	0.59×10^{-2}	2.6	0.0293
0.3	0.71×10^{-2}	2.7	0.0298
0.35	0.83×10^{-2}	2.8	0.0303
0.4	0.94×10^{-2}	2.9	0.0307
0.45	0.0104	3.0	0.0312
0.5	0.0114	3.5	0.0335
0.55	0.0124	4.0	0.0357
0.6	0.0134	4.5	0.0378
0.65	0.0143	5.0	0.04
0.7	0.0151	5.5	0.0415
0.75	0.0158	6.0	0.0429
0.8	0.0165	6.5	0.0438
0.85	0.0172	7.0	0.0446
0.9	0.0178	7.5	0.0452
0.95	0.0184	8.0	0.0457
1.0	0.019	8.5	0.0461
1.1	0.02	9.0	0.0464
1.2	0.021	9.5	0.0465
1.3	0.0219	10.0	0.0465

a. Values derived from Ref. 3.

TABLE II
 Legendre Coefficients for the D(d,n)He-3
 Center-of-Mass Neutron Angular
 Distribution Function^a

E_d (MeV)	$\underline{A_0}$	
	A_0	E_d (MeV)
0.0	0.819	1.5
0.02	0.819	2.0
0.05	0.737	2.4
0.1	0.671	3.0
0.3	0.564	3.5
0.5	0.506	5.0
0.7	0.465	7.0
1.0	0.418	10.0

E_d (MeV)	$\underline{A_2}$	
	A_2	E_d (MeV)
0.0	0.181	1.0
0.02	0.181	1.5
0.05	0.261	2.0
0.1	0.323	3.0
0.3	0.408	5.0
0.5	0.437	10.0

E_d (MeV)	$\underline{A_4}$	
	A_4	E_d (MeV)
0.0	0.0	1.2
0.03	0.0	1.5
0.05	0.002	1.8
0.1	0.006	2.0
0.35	0.035	2.5
0.55	0.066	3.0
0.8	0.108	5.25
1.0	0.142	10.0

TABLE II (Contd.)

<u>A₆</u>		<u>A₆</u>	
E _d (MeV)	A ₆	E _d (MeV)	A ₆
0.0	0.0	4.0	0.098
0.95	0.0	5.0	0.125
1.1	0.003	6.0	0.148
1.5	0.014	7.0	0.169
2.0	0.03	8.0	0.187
2.5	0.048	10.0	0.215
3.0	0.064		

<u>A₈</u>		<u>A₈</u>	
E _d (MeV)	A ₈	E _d (MeV)	A ₈
0.0	0.0	6.0	0.032
3.5	0.0	7.0	0.042
4.0	0.004	8.0	0.049
5.0	0.02	10.0	0.058

<u>A₁₀</u>		<u>A₁₀</u>	
E _d (MeV)	A ₁₀	E _d (MeV)	A ₁₀
0.0	0.0	6.0	0.008
3.5	0.0	8.0	0.011
4.0	0.002	10.0	0.014
5.0	0.005		

a. Values derived from Ref. 3.

TABLE III

Values of $Y(E_d, \theta, E_n)$ Used in Computation
of Neutron Yield from the $D(d;n,p)D$ Reaction

ED = 5.000 MEV

THETA (DEG.) =		2.5	7.5	12.5	17.5	22.5	27.5
EN (MEV)	DEN (MEV)						
.094	.187	.00E 00					
.344	.312	.00E 00					
.625	.250	.00E 00					
.875	.250	.00E 00					
1.125	.250	.00E 00					
1.375	.250	.00E 00					
1.625	.250	.00E 00					
1.875	.250	.00E 00					
2.125	.250	.00E 00					
2.375	.250	.00E 00					
2.625	.250	.00E 00					
2.875	.250	.00E 00					
3.125	.250	.00E 00					
3.375	.250	.00E 00					
3.625	.250	.00E 00					
3.875	.250	.00E 00					

ED = 5.278 MEV

THETA (DEG.) =		2.5	7.5	12.5	17.5	22.5	27.5
EN (MEV)	DEN (MEV)						
.094	.187	.00E 00					
.344	.312	.00E 00					
.625	.250	.00E 00					
.875	.250	.19E-02	.20E-02	.22E-02	.26E-02	.36E-02	.51E-02
1.125	.250	.16E-01	.18E-01	.30E-01	.39E-01	.34E-01	.32E-01
1.375	.250	.26E-01	.26E-01	.28E-01	.31E-01	.25E-01	.97E-02
1.625	.250	.22E-01	.23E-01	.21E-01	.12E-01	.29E-02	.00E 00
1.875	.250	.75E-03	.00E 00				
2.125	.250	.00E 00					
2.375	.250	.00E 00					
2.625	.250	.00E 00					
2.875	.250	.00E 00					
3.125	.250	.00E 00					
3.375	.250	.00E 00					
3.625	.250	.00E 00					
3.875	.250	.00E 00					

TABLE III (Contd.)

ED = 5.500 MEV

THETA (DEG.) =		2.5	7.5	12.5	17.5	22.5	27.5
EN (MEV)	DEN (MEV)						
.094	.187	.00E 00					
.344	.312	.00E 00					
.625	.250	.20E-02	.40E-02	.40E-02	.40E-02	.60E-02	.96E-02
.875	.250	.12E-01	.20E-01	.15E-01	.22E-01	.27E-01	.42E-01
1.125	.250	.28E-01	.44E-01	.38E-01	.52E-01	.60E-01	.84E-01
1.375	.250	.44E-01	.72E-01	.52E-01	.68E-01	.84E-01	.96E-01
1.625	.250	.48E-01	.80E-01	.52E-01	.56E-01	.76E-01	.72E-01
1.875	.250	.32E-01	.60E-01	.40E-01	.40E-01	.44E-01	.34E-01
2.125	.250	.20E-01	.40E-01	.22E-01	.22E-01	.13E-01	.18E-02
2.375	.250	.36E-02	.60E-02	.24E-02	.11E-02	.24E-03	.00E 00
2.625	.250	.00E 00					
2.875	.250	.00E 00					
3.125	.250	.00E 00					
3.375	.250	.00E 00					
3.625	.250	.00E 00					
3.875	.250	.00E 00					

ED = 5.793 MEV

THETA (DEG.) =		2.5	7.5	12.5	17.5	22.5	27.5
EN (MEV)	DEN (MEV)						
.094	.187	.00E 00					
.344	.312	.00E 00					
.625	.250	.43E-02	.84E-02	.77E-02	.78E-02	.12E-01	.19E-01
.875	.250	.22E-01	.43E-01	.28E-01	.36E-01	.52E-01	.79E-01
1.125	.250	.41E-01	.77E-01	.49E-01	.63E-01	.89E-01	.14E 00
1.375	.250	.62E-01	.12E 00	.82E-01	.11E 00	.15E 00	.21E 00
1.625	.250	.74E-01	.14E 00	.85E-01	.10E 00	.12E 00	.15E 00
1.875	.250	.68E-01	.12E 00	.83E-01	.85E-01	.92E-01	.67E-01
2.125	.250	.42E-01	.76E-01	.45E-01	.43E-01	.26E-01	.37E-02
2.375	.250	.73E-02	.12E-01	.47E-02	.22E-02	.50E-03	.00E 00
2.625	.250	.00E 00					
2.875	.250	.00E 00					
3.125	.250	.00E 00					
3.375	.250	.00E 00					
3.625	.250	.00E 00					
3.875	.250	.00E 00					

TABLE III (Contd.)

ED = 6.000 MEV

THETA (DEG.) =		2.5	7.5	12.5	17.5	22.5	27.5
EN (MEV)	DEN (MEV)						
.094	.187	.00E 00					
.344	.312	.00E 00					
.625	.250	.28E-02	.52E-02	.52E-02	.52E-02	.76E-02	.13E-01
.875	.250	.18E-01	.26E-01	.23E-01	.30E-01	.44E-01	.68E-01
1.125	.250	.41E-01	.60E-01	.50E-01	.64E-01	.90E-01	.14E 00
1.375	.250	.64E-01	.10E 00	.86E-01	.12E 00	.17E 00	.24E 00
1.625	.250	.84E-01	.12E 00	.12E 00	.15E 00	.21E 00	.27E 00
1.875	.250	.92E-01	.13E 00	.11E 00	.12E 00	.15E 00	.15E 00
2.125	.250	.84E-01	.10E 00	.96E-01	.10E 00	.10E 00	.80E-01
2.375	.250	.56E-01	.56E 00	.64E-01	.68E 00	.56E-01	.20E-01
2.625	.250	.32E-01	.32E-01	.28E-01	.20E-01	.44E-02	.00E 00
2.875	.250	.11E-01	.11E-01	.44E-02	.44E-03	.00E 00	.00E 00
3.125	.250	.20E-02	.18E-02	.00E 00	.00E 00	.00E 00	.00E 00
3.375	.250	.00E 00					
3.625	.250	.00E 00					
3.875	.250	.00E 00					

ED = 6.302 MEV

THETA (DEG.) =		2.5	7.5	12.5	17.5	22.5	27.5
EN (MEV)	DEN (MEV)						
.094	.187	.00E 00					
.344	.312	.00E 00					
.625	.250	.14E-02	.15E-02	.18E-02	.25E-02	.39E-02	.64E-02
.875	.250	.14E-01	.15E-01	.18E-01	.25E-01	.37E-01	.60E-01
1.125	.250	.41E-01	.44E-01	.52E-01	.65E-01	.94E-01	.15E 00
1.375	.250	.68E-01	.76E-01	.93E-01	.13E 00	.19E 00	.28E 00
1.625	.250	.98E-01	.11E 00	.15E 00	.21E 00	.29E 00	.40E 00
1.875	.250	.12E 00	.13E 00	.15E 00	.17E 00	.21E 00	.25E 00
2.125	.250	.13E 00	.13E 00	.15E 00	.17E 00	.18E 00	.16E 00
2.375	.250	.11E 00	.11E 00	.13E 00	.14E 00	.11E 00	.40E-01
2.625	.250	.68E-01	.67E-01	.62E-01	.40E-01	.91E-02	.00E 00
2.875	.250	.22E-01	.21E-01	.89E-02	.89E-03	.00E 00	.00E 00
3.125	.250	.46E-02	.37E-02	.00E 00	.00E 00	.00E 00	.00E 00
3.375	.250	.00E 00					
3.625	.250	.00E 00					
3.875	.250	.00E 00					

TABLE III (Contd.)

ED = 6.500 MEV

THETA (DEG.) =		2.5	7.5	12.5	17.5	22.5	27.5
EN (MEV)	DEN (MEV)						
.094	.187	.00E 00					
.344	.312	.00E 00					
.625	.250	.22E-02	.76E-02	.16E-01	.27E-02	.19E-02	.32E-02
.875	.250	.13E-01	.24E-01	.40E-01	.44E-01	.40E-01	.68E-01
1.125	.250	.36E-01	.50E-01	.76E-01	.96E-01	.12E 00	.22E 00
1.375	.250	.66E-01	.80E-01	.12E 00	.16E 00	.22E 00	.36E 00
1.625	.250	.99E-01	.11E 00	.16E 00	.21E 00	.29E 00	.42E 00
1.875	.250	.13E 00	.14E 00	.16E 00	.19E 00	.23E 00	.29E 00
2.125	.250	.14E 00	.15E 00	.16E 00	.16E 00	.18E 00	.16E 00
2.375	.250	.14E 00	.14E 00	.13E 00	.10E 00	.94E-01	.30E-01
2.625	.250	.11E 00	.99E-01	.67E-01	.25E-01	.95E-01	.77E-03
2.875	.250	.51E 00	.41E-01	.14E-01	.45E-02	.00E 00	.00E 00
3.125	.250	.14E-01	.11E-01	.25E-02	.00E 00	.00E 00	.00E 00
3.375	.250	.13E-02	.12E-02	.00E 00	.00E 00	.00E 00	.00E 00
3.625	.250	.00E 00					
3.875	.250	.00E 00					

ED = 6.709 MEV

THETA (DEG.) =		2.5	7.5	12.5	17.5	22.5	27.5
EN (MEV)	DEN (MEV)						
.094	.187	.00E 00					
.344	.312	.00E 00					
.625	.250	.30E-02	.13E-01	.31E-01	.29E-02	.00E 00	.00E 00
.875	.250	.12E-01	.33E-01	.66E-01	.63E-01	.44E-01	.98E-01
1.125	.250	.32E-01	.57E-01	.11E 00	.13E 00	.15E 00	.29E 00
1.375	.250	.64E-01	.84E-01	.14E 00	.18E 00	.24E 00	.44E 00
1.625	.250	.10E 00	.11E 00	.17E 00	.21E 00	.28E 00	.43E 00
1.875	.250	.13E 00	.14E 00	.18E 00	.21E 00	.25E 00	.33E 00
2.125	.250	.16E 00	.17E 00	.17E 00	.16E 00	.18E 00	.16E 00
2.375	.250	.17E 00	.17E 00	.13E 00	.67E-01	.73E-01	.21E-01
2.625	.250	.12E 00	.13E 00	.72E-01	.10E-01	.99E-02	.15E-02
2.875	.250	.30E-01	.61E-01	.19E-01	.50E 00	.00E 00	.30E 00
3.125	.250	.22E-01	.17E-01	.49E-02	.00E 00	.00E 00	.00E 00
3.375	.250	.26E-02	.24E-02	.00E 00	.00E 00	.00E 00	.00E 00
3.625	.250	.00E 00					
3.875	.250	.00E 00					

TABLE III (Contd.)

ED = 7.000 MEV

THETA (DEG.) =		2.5	7.5	12.5	17.5	22.5	27.5
EN (MEV)	DEN (MEV)						
.094	.187	.00E 00					
.344	.312	.00E 00					
.625	.250	.23E-02	.85E-02	.18E-01	.38E-02	.00E 00	.00E 00
.875	.250	.10E-01	.24E-01	.44E-01	.47E-01	.42E-01	.65E-01
1.125	.250	.30E-01	.43E-01	.73E-01	.99E-01	.15E 00	.24E 00
1.375	.250	.60E-01	.67E-01	.10E 00	.15E 00	.24E 00	.38E 00
1.625	.250	.96E-01	.97E-01	.13E 00	.19E 00	.30E 00	.41E 00
1.875	.250	.14E 00	.13E 00	.16E 00	.21E 00	.31E 00	.38E 00
2.125	.250	.17E 00	.16E 00	.17E 00	.20E 00	.27E 00	.29E 00
2.375	.250	.19E 00	.18E 00	.16E 00	.15E 00	.19E 00	.18E 00
2.625	.250	.19E 00	.17E 00	.14E 00	.10E 00	.96E-01	.10E 00
2.875	.250	.14E 00	.13E 00	.80E-01	.72E-01	.40E-01	.26E-01
3.125	.250	.76E-01	.84E-01	.68E-01	.36E-01	.28E-02	.00E 00
3.375	.250	.38E-01	.52E-01	.57E-01	.12E-01	.00E 00	.00E 00
3.625	.250	.13E-01	.18E-01	.12E-01	.60E-03	.00E 00	.00E 00
3.875	.250	.00E 00					

ED = 7.219 MEV

THETA (DEG.) =		2.5	7.5	12.5	17.5	22.5	27.5
EN (MEV)	DEN (MEV)						
.094	.187	.00E 00					
.344	.312	.00E 00					
.625	.250	.17E-02	.40E-02	.57E-02	.47E-02	.00E 00	.00E 00
.875	.250	.78E-02	.16E-01	.22E-01	.32E-01	.41E-01	.31E-01
1.125	.250	.28E-01	.30E-01	.40E-01	.73E-01	.14E 00	.19E 00
1.375	.250	.57E-01	.51E-01	.65E-01	.13E 00	.24E 00	.31E 00
1.625	.250	.92E-01	.79E-01	.97E-01	.18E 00	.31E 00	.39E 00
1.875	.250	.14E 00	.11E 00	.14E 00	.22E 00	.36E 00	.44E 00
2.125	.250	.18E 00	.16E 00	.18E 00	.25E 00	.37E 00	.42E 00
2.375	.250	.22E 00	.20E 00	.20E 00	.23E 00	.31E 00	.34E 00
2.625	.250	.23E 00	.21E 00	.21E 00	.20E 00	.20E 00	.20E 00
2.875	.250	.21E 00	.20E 00	.18E 00	.14E 00	.82E-01	.51E-01
3.125	.250	.15E 00	.17E 00	.14E 00	.73E-01	.56E-02	.00E 00
3.375	.250	.76E-01	.10E 00	.74E-01	.24E-01	.00E 00	.00E 00
3.625	.250	.25E-01	.37E-01	.24E-01	.12E-02	.00E 00	.00E 00
3.875	.250	.00E 00					

TABLE IV

Ratio of Scattered to Direct Neutrons
for the Gas Target Structure^a

E_d (MeV)	Percent Scattered Neutrons		
	Elastic	Inelastic	Total
2	1.08	0.52	1.6
3	0.8	0.37	1.17
4	0.6	0.25	0.85
5	0.46	0.21	0.67
6	0.35	0.16	0.51
7	0.35	0.17	0.52
8	0.4	0.15	0.55

- a. Table gives the ratio of the total scattered to direct D(d,n)He-3 neutrons for a 2.54 cm diameter disk at zero degrees and 5 cm from the gas target.

TABLE V

Deuteron Energy Loss in a Deuterium Gas Target^a

E_d (MeV)	ΔE_{dW} (MeV)	ΔE_{dG} (MeV)
3.0	0.193	0.162
3.5	0.176	0.142
4.0	0.162	0.127
4.5	0.151	0.115
5.0	0.142	0.106
5.5	0.134	0.098
6.0	0.127	0.090
6.5	0.122	0.084
7.0	0.116	0.080

a. Two centimeter long deuterium gas target cell operated at 2 atmospheres with a 2 milligram/cm² nickel window.

TABLE VI

Effect of Background Neutrons from the Gas Target
Structure in Some Typical Measurements^a

Ni-58 (n,p)Co-58

E_d (MeV)	Percent Activations Due to Background	Percent Fissions Due to Background
4.5	3.4	4.2
5.5	4.5	5.4
6.0	6.3	7.7
6.5	8.2	10
7.0	14	15

Al-27(n,p)Mg-27

E_d (MeV)	Percent Activations Due to Background	Percent Fissions Due to Background
5.0	2.4	9.5
5.5	3.7	11
6.0	5.2	13
6.5	6.1	16
7.0	7.7	20

Co-59(n,p)Fe-59

E_d (MeV)	Percent Activations Due to Background	Percent Fissions Due to Background
5.0	2.5	9.3
6.0	5.5	18
6.5	6.5	22
7.0	7.6	23

a. Ratios computed for gas cell with 2 milligram/cm² nickel window. Gas cell filled to 2 atmospheres of D₂ gas for normal irradiations and evacuated for background irradiations. Variation of fission yields for specific E_d reflect variations in beam conditions and degree of carbon buildup on the targets.

TABLE VII

Effect of the $D(d;n,p)D$ Neutrons
in Some Typical Measurements^a

Ni-58(n,p)Co-58

E_d (MeV)	Percent Contribution from $D(d;n,p)D$ Neutrons
\leq 5.0	0.0
5.5	+ 0.3
6.0	+ 3.4
6.5	+ 7.2
7.0	+ 8.9

Al-27(n,p)Mg-27

E_d (MeV)	Percent Contribution from $D(d;n,p)D$ Neutrons
\leq 5.0	0.0
5.5	+ 0.4
6.0	+ 4.5
6.5	+ 9.0
7.0	+13.2

Co-59(n,p)Fe-59

E_d (MeV)	Percent Contribution from $D(d;n,p)D$ Neutrons
\leq 5.0	0.0
6.0	+ 3.4
6.5	+ 8.0
7.0	+11.8

a. Table indicates the percent change in computed cross section when $D(d;n,p)D$ neutrons are included in reaction cross section calculations.

FIGURE CAPTIONS

Fig. 1. Gas target assembly and fission chamber used in neutron activation measurements.

(ANL Neg. No. 116-2355 Rev. 1).

Fig. 2. Schematic diagram of apparatus used in neutron activation measurements. Several variables appearing in the reaction cross section computations are indicated in this figure.

(ANL Neg. No. 116-2367).

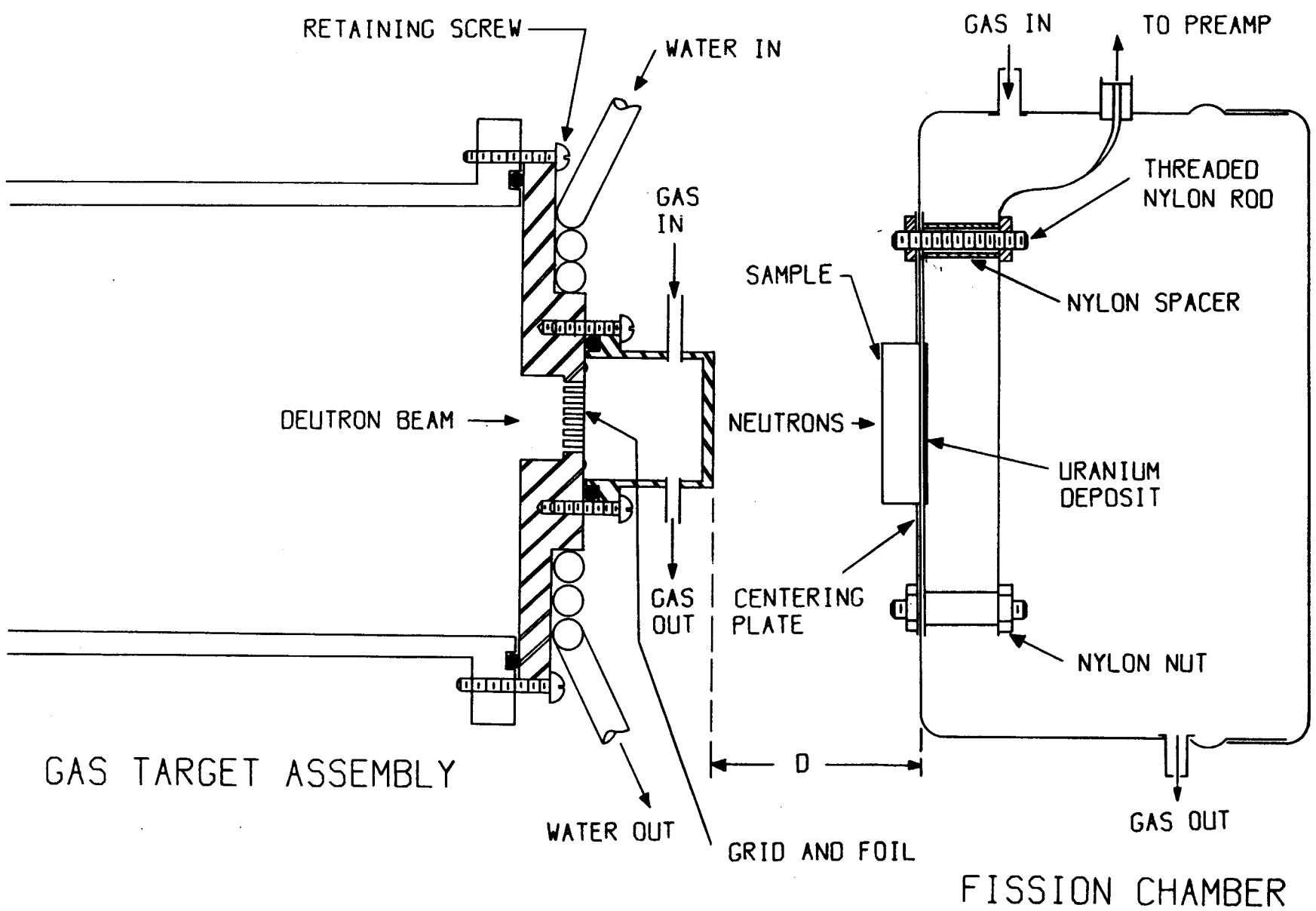


FIG. 1

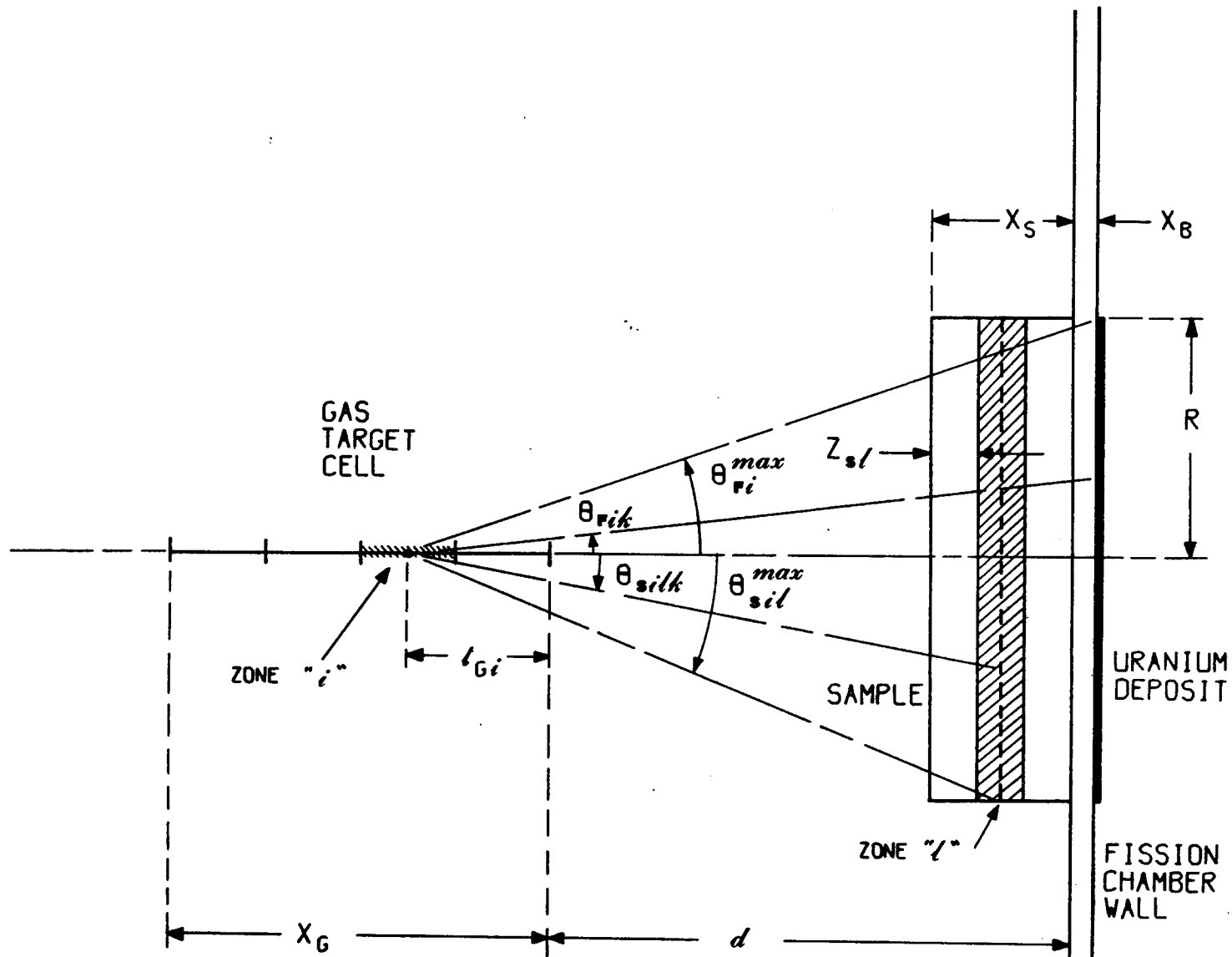


Fig. 2